

## Electrochemical Synthesis of Ferrate ( $\text{FeO}_4^{2-}$ ) in Extreme Alkaline Medium and its Application in Dye Degradation

GUNAWAN<sup>\*</sup>, N.B.A. PRASETYA and R.A. WIJAYA

Department of Chemistry, Faculty of Science and Mathematics, Diponegoro University, Semarang, Indonesia

\*Corresponding author: E-mail: [gunawan@live.undip.ac.id](mailto:gunawan@live.undip.ac.id)

Received: 9 July 2022;

Accepted: 31 October 2022;

Published online: 25 November 2022;

AJC-21067

Synthesis of ferrate ( $\text{FeO}_4^{2-}$ ) from iron plate of transformer waste electrochemically in high alkaline medium and its application for dye degradation has been carried out. The effect of parameters such as time, NaOH concentration, type of electrolyte solution and ferrate stability were studied. The ferrate solution formed is dark purple in colour with a maximum wavelength of 505 nm. The ferrate was compacted by fresh drying to produce  $\text{Na}_2\text{FeO}_4$  crystals and characterized by XRF, XRD and FT-IR techniques. The ferrate was applied to degrade methylene blue, methyl orange, rhodamine and remazol black B dyes. The results showed the highest degradation of dyestuff in methylene blue by 98% and COD reduction by 73.69% at pH 8, ferrate dose of 1.1 mg and contact time of 70 min. This shows that ferrate is an environmentally friendly material which can be used to degrade toxic dyes.

**Keywords:** Ferrate, Electrochemical synthesis, Chemical oxygen demand, Degradation, Dyes.

### INTRODUCTION

Iron scrap is one of the most widely available as metal wastes. This is due to the large amount of ferrous metal production, which reaches 92% of metal production in the world. According to data from the US Geological Survey, the total production of iron in the world in 2020 reached around 2.4 billion tons [1]. The existence of iron scrap in other forms can pose a risk to human health, so it must be recycled so as not to interfere with health and the environment. Even though behind the presence of abundant iron on earth, iron also has good potential and interesting electrochemical properties. Through two-electron transfer, iron provides a theoretically high specific capacity of  $960 \text{ mAh g}^{-1}$  and an outstanding volumetric capacity of  $7557 \text{ mAh cm}^{-3}$ , both of which are higher than zinc anodes [2]. Its redox potential of 0.44 V vs. SHE is 0.3 V higher than that of zinc, which makes for better stability.

Iron is used in various fields such as building materials, transportation equipment, food packaging materials and electronic equipments. Electronic devices are often used by humans, so they can contribute quite a lot of wastes in the form scrap. Based on data from The Global E-waste Monitor 2020, the generation of electronic waste during 2019 reached 53.6

million tons [3]. Used transformers are the result of electronic equipment waste that can be recycled. The iron contained in the used transformer has the potential to be used as an anode in the electrolysis process. The process of electrolysis of iron can produce ferrate ions in solution.

Ferrate ( $\text{FeO}_4^{2-}$ ) ions is a very strong oxidizing agent in aqueous media [4] and works as oxidants, disinfectants, coagulant, sterilizer, adsorbent and deodorizer agents [5-8]. Ferrate ions has been known as a non-toxic and environmentally friendly oxidizing agent of organic pollutants with high efficiency and low operating costs [9,10]. Spontaneous oxidation of Fe(VI) in water forms molecular oxygen. Fe(VI) oxidizes pollutants due to the chemical instability of ferrate under aqueous conditions in the normal pH range of water, which reduces Fe(VI) to Fe(III).

Several studies of ferrate synthesis have been carried out. Iron which is often used for ferrate synthesis generally comes from  $\text{Fe}(\text{NO}_3)_2$ ,  $\text{FeCl}_3$  or iron electrolysis as anode to produce iron ions [11,12]. Chen *et al.* [13] used chitosan encapsulated ferrate for removal of methyl orange dye. Villanuev *et al.* [14] reported the electrogeneration of ferrite ions under acidic conditions and its applications in the degradation of methanol yellow dye. Meanwhile, in this study, ferrate was synthesized at high

pH by electrolysis method using transformer waste iron and applied for degradation of methylene blue and methyl orange, rhodamine as well as remazol black B dyes as comparison. This research has the advantage by using materials from used transformer iron as a material for synthesis of ferrate ( $\text{FeO}_4^{2-}$ ) ions.

The electrochemical synthesis of ferrate ( $\text{FeO}_4^{2-}$ ) ions can be remarkably affected by many factors, predominantly, current density [15], electrolyte type and concentration, anode composition and temperature [16]. In this study, synthetic parameters such as time, oxidizing concentration, electrolyte type and ferrate stability were observed to determine the optimum conditions for ferrate synthesis. In addition, the effect of pH, dose of addition of ferrate, duration of degradation, comparison of effectiveness in colour degradation and chemical oxygen demand (COD) degradation of methylene blue, methylene orange, remazol black B and rhodamine dyes were also studied to determine the optimum degradation application conditions.

## EXPERIMENTAL

Iron anode plate from a used transformer was collected from the local electricity board office, whereas zinc cathode plate, sodium hydroxide, potassium hydroxide, sodium hypochlorite, methyl orange, remazol black B, methylene blue, rhodamine and sulfuric acid were procured from Merck, USA.

### Synthesis of ferrate

#### Synthesis of ferrate by electrolysis with extreme bases:

A 1.5 cm × 5 cm size of iron anode collected from the used transformer and zinc cathode plates were connected to a DC power source (Aditeg APS 3005). Electrolysis was run after immersing the two electrodes (submerged area 3 cm × 1.2 cm) into a beaker containing 50 mL of 14 M NaOH with an applied potential and current of 3 V and 4.28 A, respectively, for 60 min in an ice vessel. The electrolyzed solution was filtered using glass wool to separate the impurities. Then 10 mL of NaOCl was added to improve the stability of the ferrate. The maximum wavelength of solution was then determined using UV-Vis spectrophotometer (Genesys 10 S UV-Vis). Using a freeze-drying process, liquid sodium ferrate was frozen at -70 °C for 12 h to obtain solid  $\text{Na}_2\text{FeO}_4$ .

**Determination of electrolysis time and optimum NaOH concentration for ferrate synthesis:** The maximum ferrate concentration at a given time was used to determine the optimal electrolysis time. Meanwhile, the optimization of NaOH concentration as electrolysis solution was carried out with variations of 5, 10, 14 and 20 M. After every 5 min, 0.25 mL of sample were taken and diluted to 10 mL for measurement of ferrate concentration using a UV-Vis spectrophotometer at a maximum wavelength of 505 nm.

**Determination of electrolysis solution type on ferrate synthesis:** The effect of electrolysis solution type was carried out on a samples of 50 mL of 14M NaOH and KOH solution. After every 5 min, 0.25 mL of sample were taken and diluted to 10 mL to be measured using a UV-Vis spectrophotometer at a maximum wavelength of 505 nm.

**Determination of stability of ferrate solution:** After diluting the ferrate solution (0.5 mL) to 25 mL, absorbance

measurements at 505 nm were taken for 10 days in a row using a UV-Vis spectrophotometer. Ferrate stability was determined from the percentage degradation of ferrate concentration per day.

**Characterization of ferrate:** The dried ferrate solid was analyzed using X-ray fluorescence (PANalytical XRF), X-ray diffractometer (Shimadzu XRD-6100/7000) and FTIR spectrophotometer (Shimadzu IRPRESTIGE 21).

### Application of ferrate for degradation of methylene blue

**Determination of maximum wavelength of methylene blue:** A UV-Vis spectrophotometer at a wavelength of 200-800 nm was used to scan 2.5 mL sample of 100 mg/L methylene blue dye solution. The maximum wavelength was determined from the largest absorbance value.

**Effect of pH:** By mixing 10 mL of methylene blue (10 mg/L) and 0.15 mL (4.6 mg/mL) ferrate at a pH range of 7 to 11, the optimum pH for the decomposition of methylene blue by ferrate was determined. The mixture was stirred for 30 min and after that the concentration of degraded methylene blue was determined by UV-vis spectrophotometer.

**Effect of ferrate dose:** The influence of ferrate dosage on methylene blue degradation was investigated using 10 mL of 10 mg/L methylene blue solution. The methylene blue solution was added with a variation of 0.21, 0.42, 0.63, 0.84, 1.1 mg ferrate at the optimum pH degradation and homogenized with a stirrer for 15 min and then measured the absorbance of the solution.

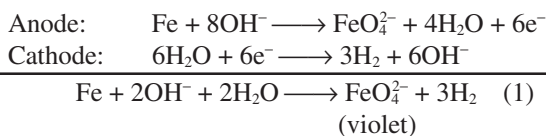
**Effect of time:** The effect of degradation time on methylene blue was carried out on a sample of 10 mL of methylene blue (10 mg/L). The methylene blue solution was then added with 0.15 mL of ferrate (4.6 mg/mL) at pH 8, then the solution was homogenized with a magnetic stirrer for 75 min. After every 5 min interval, the absorbance of the sample was measured.

**Comparison of degradation of methylene blue with methyl orange, remazol black B and rhodamine dyes:** The effect of different dyes (methylene blue, methyl orange, remazol black B and rhodamine) on the ferrate degradation ability was investigated by varying the dye sample. Each dye (10 mg/L) was mixed with 0.15 mL of ferrate (4.6 mg/mL) at pH 8 and stirred for 15 min. The absorbance was measured using a UV-Vis spectrophotometer at the maximum wavelength of methylene blue (664 nm), methyl orange (467 nm), remazol black B (595 nm) and rhodamine B (554 nm). The decrease of COD values were determined before and after the treatment with ferrate.

## RESULTS AND DISCUSSION

**Synthesis of ferrate by electrolysis:** Synthesis of ferrate by electrolysis in highly alkaline medium was carried out using used transformer iron plate electrode as anode, zinc as cathode and 14 M NaOH solution as electrolyte. This method is the simplest way to obtain sodium ferrate in solution free of impurities. Furthermore, electrolysis was carried out with a constant voltage of 4 V and a current reading of 4.28 A.

The oxidation-reduction reaction occurs during electrolysis of iron plate (eqn. 1) is shown as follows:



At the initiation of the electrolysis process, the colour of the solution changes from colourless to violet, indicating the formation of ferrate ions. After a specific period of time, a dark purple solution will form and the electrode will become black due to passivation [17]. The resulting  $\text{Na}_2\text{FeO}_4$  solution was filtered using glass wool to remove impurities in the solution. The ferrate solution obtained was stored in a closed container and dark in colour to prevent its reduction back to  $\text{Fe}^{3+}$  as shown in the following reaction [18]:



The solutions were then characterized and quantified, using a UV-Vis spectrophotometer. Fig. 1 shows the spectra of the synthesized ferrate and shows the maximum absorption peak at a wavelength of 505 nm [19-21]. The absorbance in Fig. 1 is 0.518, so with a 10-fold dilution factor, the ferrate concentration is actually determined by using Lambert-Beer law equation of 735 mg/L.

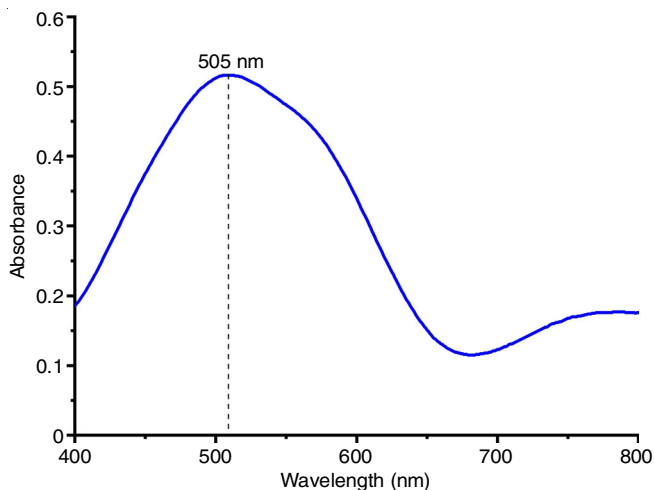


Fig. 1. Spectra of ferrate solution resulting from electrolysis

**Effect of electrolysis time and NaOH concentration on the ferrate synthesis:** The obtained ferrate concentration increases with increasing electrolysis time until the maximum time limit is shown by a reduction (Fig. 2). Due to the reduction of ferrate to form iron hydroxide deposits in aqueous media [22], which causes a drop in ferrate production performance.

At each concentration, the optimum electrolysis time may vary. The longer the optimal production period, the more ferrate is produced when using a concentrated NaOH solution. The optimum times for samples with 5, 10, 14 and 20 M NaOH were 70, 55, 75 and 130 min, respectively, as shown in Fig. 3. The concentration of NaOH affects the increase in the concentration of ferrate produced. However, compared to NaOH 10, 14, and 20 M, 5 M looks the most inclined; hence, the greatest ferrate produced is approximately 500 mg/L. Meanwhile, results from highly alkaline solution conditions at 10, 14 and 20 M concentrations produced an increasing graph pattern

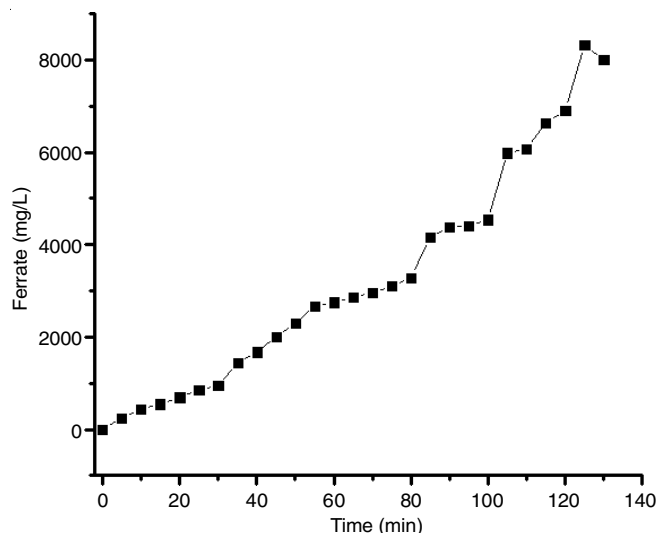


Fig. 2. Effect of time on the electrolysis of ferrate with 20 M NaOH solution

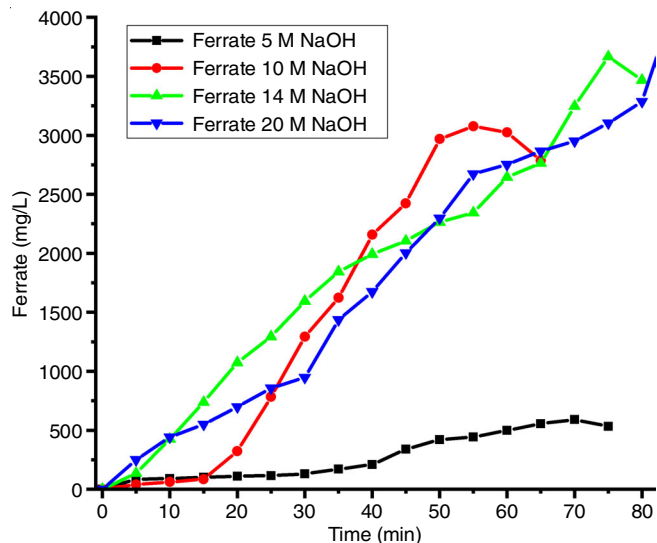


Fig. 3. Effect of time and NaOH concentration on ferrate concentration

with nearly the same slope. However, as can be seen from Fig. 3, using 14 M NaOH results in a more stable.

These findings suggested that a longer formation time and a higher ferrate concentration correlated with the higher NaOH concentrations. This is due to the fact that the oxidizing ability increases with increasing NaOH concentration. However, the amount of Fe converted to ferrate increases with the length of time.

**Effect of type of electrolysis solution:** Fig. 4 demonstrates that the amount of ferrate produced varied depending on the type of alkaline solution employed. As a result, solutions of KOH and NaOH at the same concentration of 14 M exhibit different graphic patterns. At a maximum time of 75 min, electrolysis with NaOH solution resulted a high ferrate with a yield of 3600 mg/L. Meanwhile, KOH gives a maximum ferrate yield of around 1000 mg/L at 65 min. So, it is observed that the electrolysis results are more optimum with NaOH than KOH.

This result is influenced by the oxidizing ability of the alkaline solution used as an electrolyte. The basic strength of



**XRF studies:** The presence of ferrate in the form of  $\text{Na}_2\text{FeO}_4$  is confirmed by the XRF results (Table-1). The majority of Fe is found in the oxide state as  $\text{FeO}_4^{2-}$ . There are also other elements present such as Cl due to NaOCl used and Zn from the cathode plate.

Element	Weight (%)	Element	Weight (%)
Na	5.1802	Fe	0.0237
Si	0.2461	Zn	0.0519
Cl	0.8394	Ag	0.0545
K	0.0204	Balance (iron oxide)	93.574
Ca	0.0099		

**IR studies:** A sharp peak in the fingerprint region showing the characteristic strain vibration of Fe-O bonds in ferrate appears at  $624\text{ cm}^{-1}$ ,  $779\text{ cm}^{-1}$ ,  $879\text{ cm}^{-1}$  and confirms the presence of a typical Fe-O bond of  $\beta\text{-FeO(OH)}$  [27] and  $\alpha\text{-FeO(OH)}$  [28] in sodium ferrate(VI) salt. Additionally, a peak at  $1640\text{ cm}^{-1}$  appears as the  $-\text{OH}$  vibrational strain of  $\text{H}_2\text{O}$  [29,30]. The absorption at  $1434\text{ cm}^{-1}$  is a characteristic of the stretching vibration of the C-O bond, which corresponds to the  $\text{CO}_2$  peaks in the atmosphere [31]. The peaks obtained between  $2886$  and  $3573\text{ cm}^{-1}$  are ascribed to the H-O bonds of water [32] (Fig. 7). The crystalline conditions may be the cause of little variation in the chemical shift of the functional groups of the product compared to the literature [19] (Table-2).

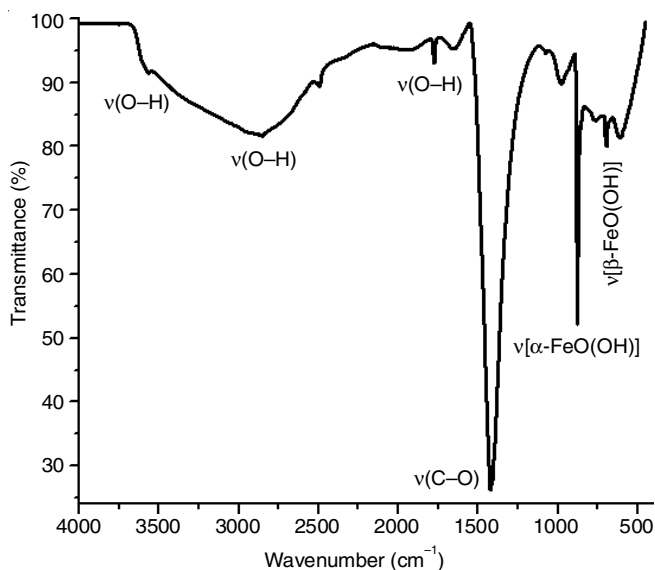


Fig. 7. IR spectra of electrolyzed ferrate

### Degradation of methylene blue

**Determination of maximum wavelength:** The wavelength of methylene blue was carried out by UV-Vis spectrophotometer at 200-800 nm as shown in Fig. 8. According to the findings, there were three absorbance maxima around 296.5, 613 and 664 nm. For the visible region, the maximum peak results in 664 nm region. In order to measure the variations in methylene blue concentration both before and after treatment, the visible maximum wavelength was used.

TABLE-2  
KEY IR BANDS ( $\text{cm}^{-1}$ ) OF FUNCTIONAL GROUPS PRESENT IN SYNTHESIZED FERRATE

Functional group	Wavelength ( $\text{cm}^{-1}$ )
O-H	3573
H-O-H	2886
O-H	1640
C-O	1434
Fe-O ( $\alpha\text{Fe-OOH}$ )	879
Fe-O ( $\alpha\text{Fe-OOH}$ )	779
Fe-O ( $\beta\text{Fe-OOH}$ )	624

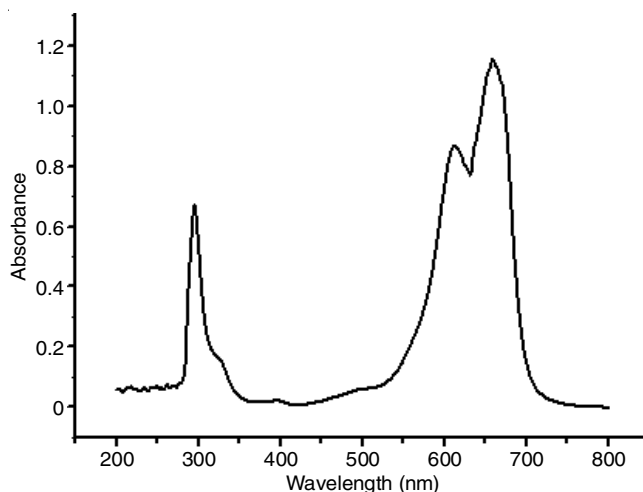


Fig. 8. Spectra of the maximum wavelength of methylene blue

**Calibration curve:** The methylene blue sample before being treated was calibrated at a concentration of 1 up to 5 mg/L. The calibration curve shows that the absorbance measurement, which was performed at a wavelength of 664 nm, has good linearity up to a concentration of 5 mg/L with an  $R^2$  value of 0.9941 (Fig. 9).

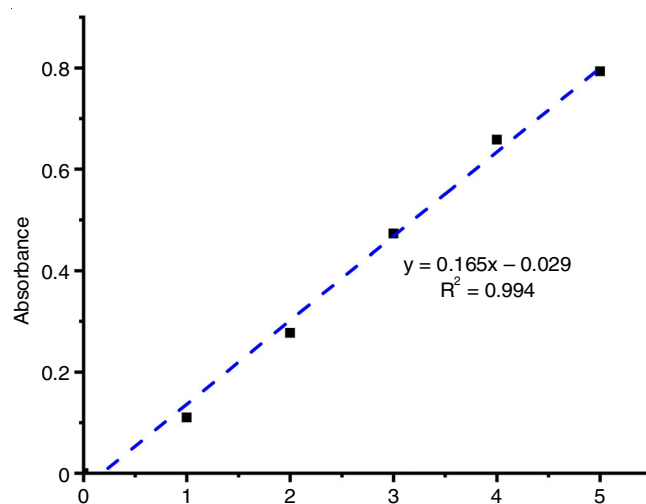


Fig. 9. Methylene blue calibration curve

**Effect of pH:** Ferrate and methylene blue were conditioned at alkaline pH levels between pH 7 and pH 11, in order to determine the optimum pH value for the degradation. This is

due to the strong oxidizing properties of ferrate at alkaline pH, where it is more stable than at acidic pH, when it will oxidize water [19].

Fig. 10 demonstrates that a decrease of 98% occurs at pH 8, which is the optimum pH for methylene blue degradation, which indicated that ferrate is more stable under an alkaline pH than an acidic. This result is consistent with the work of Li *et al.* [33]. The predominant species in acidic environments are  $\text{HFeO}_4^-$ ,  $\text{H}_3\text{FeO}_4^+$ ,  $\text{H}_2\text{FeO}_4$  and  $\text{HFeO}_4^-$ . The ferrite species involved under neutral conditions were  $\text{HFeO}_4^-$  and  $\text{FeO}_4^{2-}$ , with  $\text{HFeO}_4^-$  species being the dominating one.  $\text{HFeO}_4^-$  and  $\text{FeO}_4^{2-}$  species are present under the alkaline solution conditions, but  $\text{FeO}_4^{2-}$  is more prevalent [18,34].

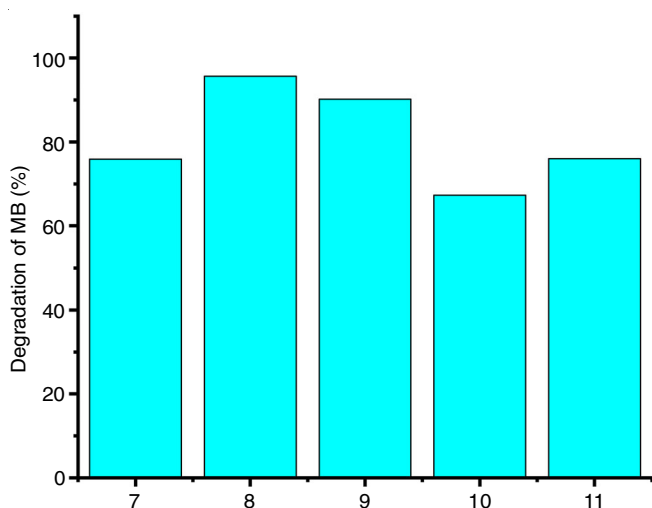


Fig. 10. Effect of pH on methylene blue degradation with ferrate

**Effect of ferrate dose:** The effect of ferrate dose on methylene blue degradation are shown in Fig. 11. When ferrate dose increases, the number of mg/g methylene blue consumed decreases (Fig. 11a). An increase in the degradation percentage of methylene blue occurs as the dose of ferrate increased (Fig.

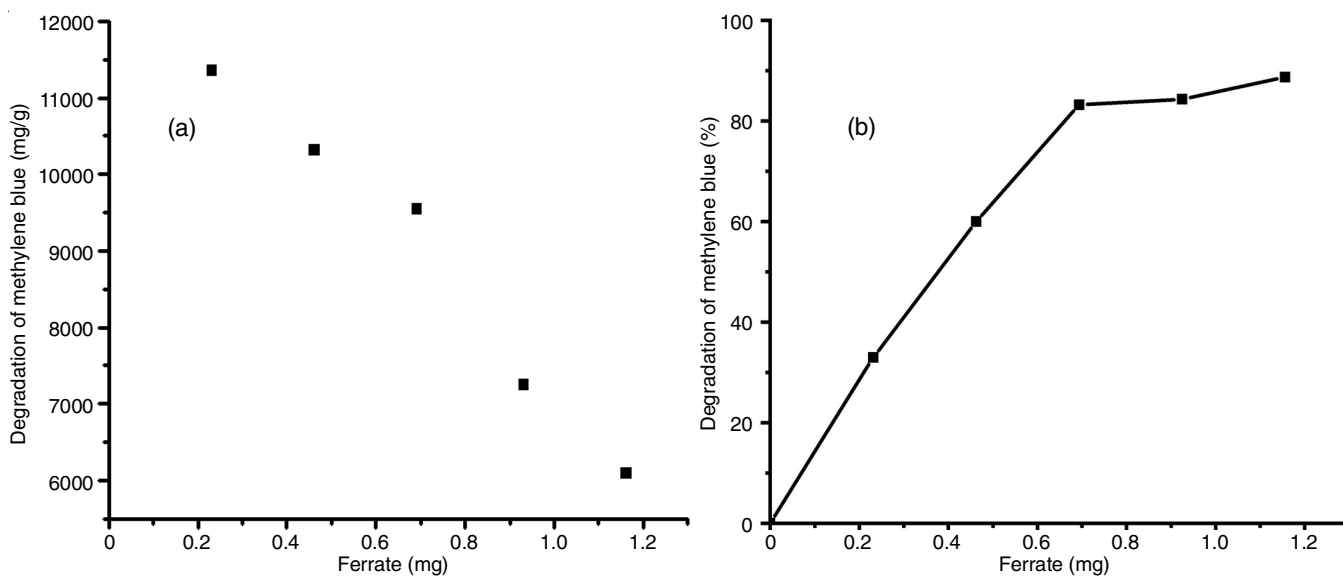


Fig. 11. Effect of ferrate dose on concentration degradation (a) and percent degradation of methylene blue (b)

11b). However, the optimum addition dose for the degradation of methylene blue is 1.1 mg with a degradation ability of 72.5%. The higher dose of ferrate addition in the ratio of ferrate and methylene blue resulted in the higher degradation ability. However, an excessive dose of ferrate(VI) ion reduced the efficiency of degradation due to the decomposition of ferrate(VI) ion [35].

**Effect of time:** The decomposition of the treated methylene blue was carried out with 10 mL of 10 mg/L methylene blue containing 0.15 mL of ferrate and stirred for a predetermined time. Fig. 12a demonstrates that the decomposition increases as the time increases to 70 min, with the maximum degradation percentage around 75%. The reaction between ferrate and methylene blue can therefore be observed to follow an order of 1, which is shown by an excellent linearity that is close to 1 ( $R^2 = 0.99$ ) (Fig. 12b). This conclusion is consistent with the literature, which indicates that methylene blue decayed more quickly the longer the degradation time [18].

**Degradation of methylene blue with methyl orange, remazol black B and rhodamine dyes:** Fig. 13 shows that ferrate can act as a dye degrading agent. The degradation of methylene blue gave the highest percentage of degradation (89%) followed by methyl orange, remazol black B and rhodamine dyes. The reason is attributed due to the structure of the dyes, which can be easily degraded by ferrate. The more complicated the structure, the longer the degradation process will occur. On the other hand, the structure of remazol black B and rhodamine dyes is more complicated. The compound is an azo dye with two azo chromophores (one is the hydrazone tautomer); the auxochromes are sulfone, amine and sulfonate groups so that the greater the steric hindrance that blocks or inhibits the breaking of the chromophore group bonds and the smaller the percentage of degradation [36].

**Measurement of COD reduction of dyes after treated by ferrate:** Table-3 shows the results of the chemical oxygen demand (COD) analysis for dyes before and after treatment with ferrate. It is observed that the presence of more comp-

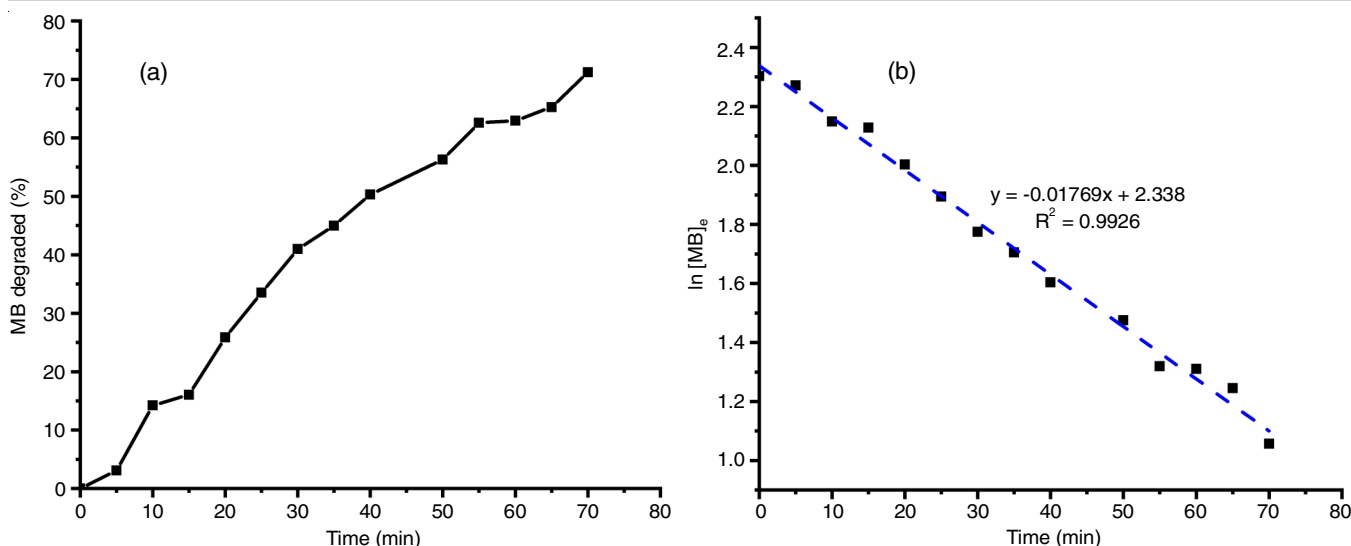


Fig. 12. Effect of time on methylene blue degradation by ferrate (a) and methylene blue degradation kinetics (b)

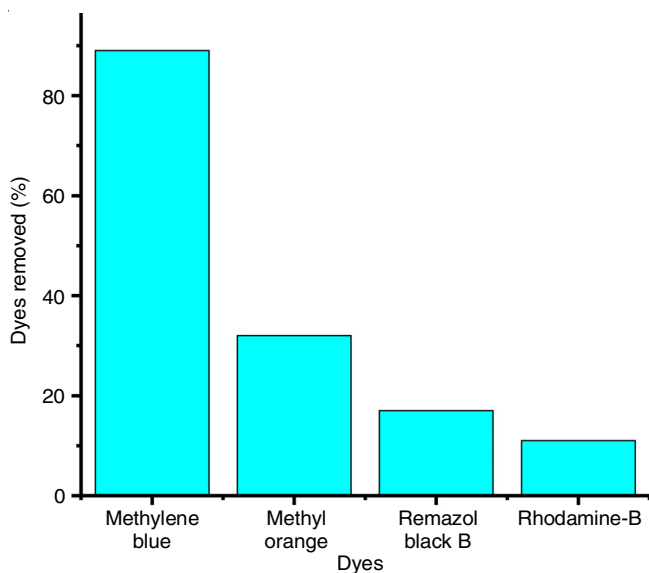


Fig. 13. Comparison of dye degradation (methylene blue, methyl orange, remazol black B and rhodamine-B) by ferrate

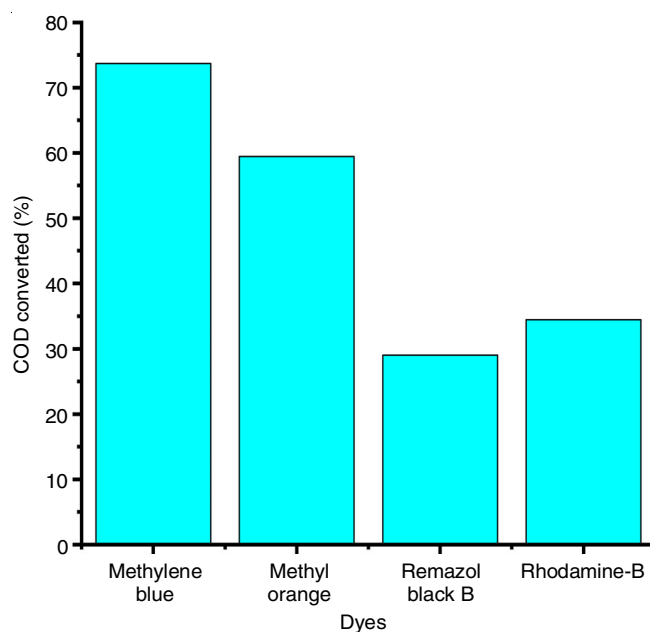


Fig. 14. Comparison of COD degradation (methylene blue, methyl orange, remazol black B, rhodamine-B) by ferrate

TABLE-3  
COMPARISON DATA OF COD DEGRADATION  
IN PRESENCE OF DIFFERENT DYES SAMPLES

Dyes	COD		Degradation (%)
	Initial	Final	
Methylene blue	112.44	29.588	73.69
Methyl orange	59.175	24.000	59.44
Rhodamine-B	98.509	64.571	34.45
Remazol black B	75.187	53.358	29.03

licated colour pigment structure will slow down the decrease in the COD value. Since, among the tested dyes, methylene blue has the simplest structure so that it provides the best COD reduction of 73.69% compared to methyl orange, remazol black B and rhodamine as shown in Fig. 14. Since oxidation of pollutants using ferrate(VI) does not generate any toxic and mutagenic by products, it is known as a green technology and ferrate(VI) is known as green chemical.

## Conclusion

Electrochemical synthesis of ferrate ( $\text{FeO}_4^{2-}$ ) using iron plate transformer waste and its applications in the dye degradation have been achieved successfully. The concentration of ferrate obtained depends on the length of time for electrolysis and the concentration of NaOH used. Characterization of ferrate with XRF, XRD and IR confirmed the typical properties of ferrate. The methylene blue degradation was measured at the maximum wavelength at 664 nm and the highest percentage of degradation of methylene blue dye of 98% and COD reduction of 73.69% were achieved with the optimum conditions obtained at pH 8, ferrate dose of 1.1 mg and time of 70 min. This work demonstrated that ferrate(VI) is acted as green material, which is safe for the environment and can be employed to decompose the toxic dyes.

## ACKNOWLEDGEMENTS

This research was funded by Riset Pengembangan dan Penerapan (RPP) Universitas Diponegoro 2021 with contract number 185-42/UN7.6.I/PP/2021.

## CONFLICT OF INTEREST

The authors declare that there is no conflict of interests regarding the publication of this article.

## REFERENCES

- U.S. Geological Survey, Mineral Commodity Summaries 2020, U.S. Geological Survey, USA, p. 200 (2020).
- X. Wu, A. Markir, Y. Xu, C. Zhang, D.P. Leonard, W. Shin and X. Ji, *Adv. Funct. Mater.*, **29**, 1900911 (2019); <https://doi.org/10.1002/adfm.201900911>
- V. Forti, C.P. Baldé, R. Kuehr and G. Bel, The Global E-waste Monitor 2020 Quantities, Flows, and the Circular Economy Potential (2020).
- V.K. Sharma, L. Chen and R. Zboril, *ACS Sustain. Chem. Eng.*, **4**, 18 (2016); <https://doi.org/10.1021/acssuschemeng.5b01202>
- A. Mulyengabe and C. Zvinowanda, *Braz. J. Anal. Chem.*, **6**, 40 (2019); <https://doi.org/10.30744/brjac.2179-3425.RV-19-2019>
- S.T. Mcbeath, D.P. Wilkinson and N.J.D. Graham, *J. Environ. Chem. Eng.*, **8**, 103834 (2020); <https://doi.org/10.1016/j.jece.2020.103834>
- D. Majid and I.K. Kim, *J. Environ. Eng.*, **144**, 04018093 (2018); [https://doi.org/10.1061/\(ASCE\)EE.1943-7870.0001440](https://doi.org/10.1061/(ASCE)EE.1943-7870.0001440)
- S. Barisci, F. Ulu, H. Särkkä, A. Dimoglo and M. Sillanpää, *Int. J. Electrochem. Sci.*, **9**, 3099 (2014).
- S. Barisci, *J. Water Process Eng.*, **20**, 84 (2017); <https://doi.org/10.1016/j.jwpe.2017.10.005>
- J.Q. Jiang and B. Lloyd, *Water Res.*, **36**, 1397 (2002); [https://doi.org/10.1016/S0043-1354\(01\)00358-X](https://doi.org/10.1016/S0043-1354(01)00358-X)
- F. Zeng, C. Chen and X. Huang, *Chemosphere*, **241**, 125124 (2020); <https://doi.org/10.1016/j.chemosphere.2019.125124>
- E.A. Maghraoui, A. Zerouale and M. Ijjaali, *Adv. Mater. Phys. Chem.*, **5**, 10 (2015); <https://doi.org/10.4236/amcp.2015.51002>
- B.-Y. Chen, H.-W. Kuo, V.K. Sharma and W. Den, *Sci. Rep.*, **9**, 18268 (2019); <https://doi.org/10.1038/s41598-019-54798-4>
- M. Villanueva, A. Hernandez, J.M. Peralta-Hernandez, E.R. Bandalab and M.A. Quiróz, *ECS Trans.*, **15**, 411 (2008); <https://doi.org/10.1149/1.3046657>
- J.Q. Jiang, N. Graham, C. Andre, G.H. Kelsall and N. Brandon, *Water Res.*, **36**, 4064 (2002); [https://doi.org/10.1016/S0043-1354\(02\)00118-5](https://doi.org/10.1016/S0043-1354(02)00118-5)
- Z. Ding, C. Yang and Q. Wu, *Electrochim. Acta*, **49**, 3155 (2004); <https://doi.org/10.1016/j.electacta.2004.01.031>
- S.S. Sedeh, E. Saebnoori, A. Talaiekhazani, M.A. Fulazzaky, M. Roestamy and A.M. Amani, *Plasma Chem. Plasma Process.*, **39**, 769 (2019); <https://doi.org/10.1007/s11090-019-09989-2>
- Gunawan, N.B.A. Prasetya, A. Haris and F. Febriliani, *J. Phys.: Conf. Series*, **1943**, 012181 (2021); <https://doi.org/10.1088/1742-6596/1943/1/012181>
- A. Mulyengabe, C. Zvinowanda, J. Ramontja and J.N. Zvimba, *Water*, **13**, 2619 (2021); <https://doi.org/10.3390/w13192619>
- P.C.W. Cheung, D.R. Williams, J. Barrett, J. Barker, D.W. Kirk, D.R. Barrett, J. Barker, J. Kirk, K.J. Paeng and A. Pettignano, *Molecules*, **26**, 5266 (2021); <https://doi.org/10.3390/molecules26175266>
- Z. Luo, M. Strouse, J.Q. Jiang and V.K. Sharma, *J. Environ. Sci. Health Part A Tox. Hazard. Subst. Environ. Eng.*, **46**, 453 (2011); <https://doi.org/10.1080/10934529.2011.551723>
- A.E. Maghraoui, A. Zerouale, M. Ijjaali and M. Sajieddine, *Adv. Mater. Phys. Chem.*, **3**, 83 (2013); <https://doi.org/10.4236/amcp.2013.31013>
- M. Azhar, J. Efendi, E. Sofyeni, R.F. Lesi and S. Novalina, *Eksakta*, **1**, 1 (2010).
- A. Talaiekhazani, M.R. Talaei and S. Rezanian, *J. Environ. Chem. Eng.*, **5**, 1828 (2017); <https://doi.org/10.1016/j.jece.2017.03.025>
- M. Koltypin, S. Licht, I. Nowik, R.T. Vered, E. Levi, Y. Gofer and D. Aurbach, *J. Electrochem. Soc.*, **153**, A32 (2006); <https://doi.org/10.1149/1.2128121>
- G. Gunawan, A. Haris, N.B.A. Prasetya, E. Pratista and A. Amrullah, *Indones. J. Chem.*, **21**, 1397 (2021); <https://doi.org/10.22146/ijc.64824>
- S. Bashir, R.W. McCabe, C. Boxall, M.S. Leaver and D. Mobbs, *J. Nanopart. Res.*, **11**, 701 (2009); <https://doi.org/10.1007/s11051-008-9467-z>
- B. Yuan, J. Xu, X. Li and M.L. Fu, *Chem. Eng. J.*, **226**, 181 (2013); <https://doi.org/10.1016/j.cej.2013.04.058>
- L. Macera, G. Taglieri, V. Daniele, M. Passacantando and F. D'orazio, *Nanomaterials*, **10**, 323 (2020); <https://doi.org/10.3390/nano10020323>
- B.S. Zhu, Y. Jia, Z. Jin, B. Sun, T. Luo, L.T. Kong and J.H. Liu, *RSC Adv.*, **5**, 84389 (2015); <https://doi.org/10.1039/C5RA15619J>
- E. Martinez-Tamayo, A. Beltrán-Porter and D. Beltrán-Porter, *Thermochim. Acta*, **97**, 243 (1986); [https://doi.org/10.1016/0040-6031\(86\)87024-1](https://doi.org/10.1016/0040-6031(86)87024-1)
- M.G. Peleyeju, E.H. Umukoro, L. Tshwenya, R. Moutloali, J.O. Babalola and O.A. Arotiba, *RSC Adv.*, **7**, 40571 (2017); <https://doi.org/10.1039/C7RA07399B>
- C. Li, X.Z. Li and N.A. Graham, *Chemosphere*, **61**, 537 (2005); <https://doi.org/10.1016/j.chemosphere.2005.02.027>
- C. Luo, M. Feng, V.K. Sharma and C.-H. Huang, *Chem. Eng. J.*, **388**, 124134 (2020); <https://doi.org/10.1016/j.cej.2020.124134>
- V.K. Sharma, *J. Environ. Manage.*, **92**, 1051 (2011); <https://doi.org/10.1016/j.jenvman.2010.11.026>
- D.R. Waring and G. Hallas, *The Chemistry and Application of Dyes*, New York: Plenum Press (1990).